Available online at www.sciencedirect.com
ScienceDirect
Chemical Engineering and Processing 47 (2008) 799–815
Chemical Engineering and Processing Process Intensification
www.elsevier.com/locate/cep

On the gas expansion and gas hold-up in vertical slugging columns—A simulation study

T.S. Mayor, A.M.F.R. Pinto, J.B.L.M. Campos *

Centro de Estudos de Fenómenos de Transporte, Departamento de Engenharia Química, Faculdade de Engenharia da Universidade do Porto, Rua Dr. Roberto Frias, 4200-465 Porto, Portugal

Received 13 June 2006; received in revised form 24 November 2006; accepted 16 January 2007
Available online 30 January 2007

Abstract

A study on the gas phase expansion and gas hold-up occurring in free bubbling vertical slug flow is reported. A slug flow simulator (SFS) supported by air–water experimental data was used for this purpose. The study was accomplished by implementing in the simulator the gas phase expansion along the column. Effects over bubble lengths and bubble velocities were considered. The flow in 6.5 and 20 m long columns with internal diameter of 0.032 m was simulated. Expansion of gas phase along the column is shown to slightly decrease the occurrence of bubble coalescence. Liquid free surface oscillations (due to bubble burst events and continuous inlet of liquid and gas in the column) were found to affect the expansion of the gas phase, especially for high gas flow rates. The gas phase expansion for different outlet column configurations was studied. The use of a high and large cross sectional tank (to dampen free surface oscillations) is shown not to assure a permanent expansion rate of the gas phase. Simulations with and without gas expansion along the column were compared for the computation of average flow parameters. Approximate approaches (with constant U_G, corrected for the mid-column pressure) were found suitable for the prediction of the average slug length and gas hold-up. Those approaches are, however, inadequate for the computation of the average bubble length and velocity along the vertical coordinate of the column.

Keywords: Gas expansion rate; Gas hold-up; Numerical flow simulation; Slugging flow

1. Introduction

Gas–liquid mixtures flow in pipes in different flow patterns, which depend on flow rates, fluid properties, pipe diameter, inclination and configuration. Slug flow is one of these flow patterns and can be characterized by the flowing of long bubbles (known as Taylor bubbles) occupying most of column cross sectional area, separated by more or less aerated liquid plugs (termed slugs). It is a complex, irregular and intermittent phenomenon that can be found in several engineering applications (various types of reactors, membrane processes or extraction and transportation of hydrocarbons, just to mention a few) and even in natural phenomena (e.g. volcanic events).

Much of the primary modelling of slug flow was based on the early works of Dumitrescu [1], Davies and Taylor [2] and Nicklin et al. [3]. They set the bases for the first understanding of two-phase slug flow pattern. Several works followed focussing different aspects of such flow pattern (e.g. [4–6]).

The numerical simulation of two-phase vertical slug flow pattern has been attempted by several researchers (e.g. [7–9]). It serves as a tool for the study of the influence of several phenomena over the development of the flow, as well as an outcome predictor for any process/application in which this flow occurs. The usual approach requires the input of bubble-to-bubble interaction correlations relating the trailing bubble velocity to the length of the liquid slug ahead of the bubble. Different interaction correlations have been proposed (e.g. [8–10]) depending, for instance, on experimental conditions, fluid properties, flow regimes, etc. The simulation of slug flow pattern is often achieved, however, without accurate implementation of the gas phase expansion along the column (in terms of effect over bubble length and over bubble velocity). Two workarounds to address this problem are often implemented. The simplest one involves performing the flow simulation based on gas related parameters given at ambient pressure (e.g. [7,8]). A more elaborate approach involves correcting those parameters for the

* Corresponding author. Tel.: +351 225081692; fax: +351 225081449.
E-mail address: jmc@fe.up.pt (J.B.L.M. Campos).

0255-2701/$ – see front matter © 2007 Elsevier B.V. All rights reserved.
doi:10.1016/j.cep.2007.01.031

pressure at the middle of the column (e.g. [11]). These are, nevertheless, approximate approaches which comprise limitations that should be considered while elaborating on data obtained in that way. In addition, there can be operating conditions whose simulation may not produce reasonable results when using such approximate approaches (for instance regarding flow simulation in long columns). There is thus a need for input in this area.

Two-phase flows are known to play a relevant role in volcanic events. Slug flow is believed, for instance, to be responsible for Strombolian eruptions at basaltic volcanoes [12]. There are also reports associating bubble coalescence and rise to both tremor and eruption seismic signals (e.g. [13]). In addition, bubble formation, ascent and their bursting at the surface are often related to strong pressure oscillations during volcanic events [14]. But these issues are also relevant for Industry in terms of the structural integrity of facilities (for instance in hydrocarbon and natural gas extraction plants). Thus, the implementation of the gas phase expansion in a slug flow simulator can be an asset to promote a deeper understanding of the flow dynamics at the source of those phenomena.

The main goal of this work is to provide information on the influence of the gas phase expansion over the evolution of the slug flow pattern in vertical columns. An algorithm for implementation of gas phase expansion along the column is proposed and issues like column outlet configuration and its influence on gas expansion rate, the pressure and bubble velocity oscillations and the gas hold-up inside the column are addressed.

2. Experimental work

A series of air–water co-current slug flow experiments [10] were performed in a 6.5 m long acrylic vertical column (0.032 m internal diameter). An image analysis technique [15] was used to collect data on the flow pattern characteristics, at two vertical coordinates (3.25 and 5.40 m from the base of the column) and for several superficial gas and liquid velocities (U_G and U_L up to 0.26 and 0.20 m/s, respectively). The operating conditions were designed to have turbulent regime in the main liquid and in the near-wake bubble region. Two types of approaches were pursued while scrutinizing the flow frames: the *moving-point data analysis* and the *fixed-point data analysis*. The former allowed the establishment of an empirical bubble-to-bubble interaction curve for velocity, governing the approach and coalescence of consecutive bubbles, and the latter allowed to gather information on bubble characteristics (length, velocity, distance) at a given vertical coordinate.

Similar bubble-to-bubble interaction curves (velocity-wise) were obtained at the two vertical coordinates tested, for all the superficial gas and liquid velocities studied. The obtained average bubble-to-bubble interaction curve is shown in Fig. 1a, together with the best fit equation. The form and parameters of this equation are shown below:

$$\frac{U_i^{\text{trail}}}{U_{\text{B}}^{\text{exp}}} = 1 + 2.4\,\text{e}^{-0.8(h_{\text{s},i-1}/D)^{0.9}} \tag{1}$$

where D is the column internal diameter (ID), U_i^{trail} refers to the velocity of the trailing bubble i, flowing behind a liquid slug of length $h_{\text{s},i-1}$ and $U_{\text{B}}^{\text{exp}}$ is the experimental average upward bubble velocity in undisturbed conditions. The estimates of $U_{\text{B}}^{\text{exp}}$ are plotted against the superficial mixture velocity ($U_{\text{M}} = U_{\text{L}} + U_{\text{G}}$) in Fig. 1b, together with the Nicklin [3] predictions for co-current flow in turbulent regime. The Nicklin correlation is of the form:

$$U_{\text{B}} = U_\infty + CU_{\text{M}} \tag{2}$$

where U_∞ is the drift velocity and C an empirical parameter related to the velocity profile in the liquid. The drift velocity in a 0.032 m ID column equals 0.196 m/s (inertial controlled regime [6]) whereas parameter C equals 1.2 for turbulent regime in the liquid [3]. The agreement between the experimental estimates of $U_{\text{B}}^{\text{exp}}$ and the Nicklin predictions (Eq. (2)) is evident.

Besides the relations (1) and (2), crucial inputs for the simulation of the slug flow pattern, the experimental study allowed to collect a vast amount of data on the flow characteristics at the two vertical coordinates tested. These data provided the means for the validation of the simulation results (Section 4.1). The following section describes the assumptions and approaches of the slug flow simulator.

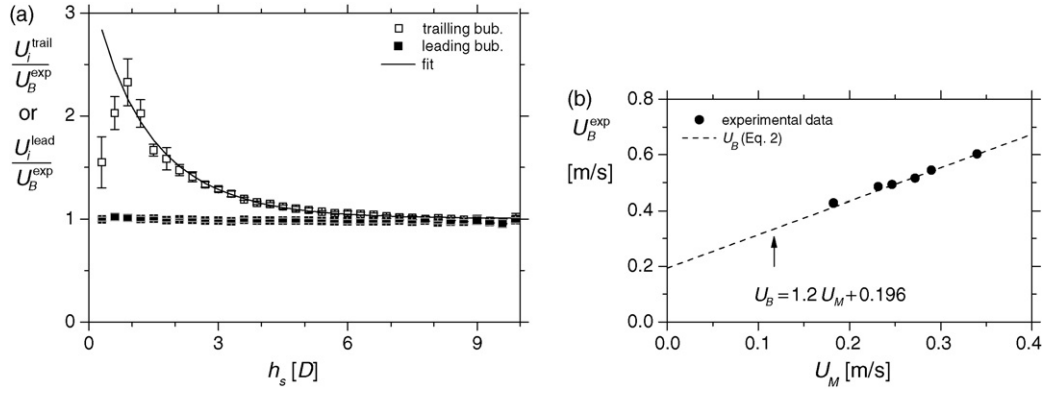

Fig. 1. (a) Average bubble-to-bubble interaction curve with 95% confidence intervals (vertical coordinates: 3.25 and 5.4 m) and (b) experimental average upward bubble velocity plotted against U_{M} after correction for vertical coordinate 5.4 m; internal diameter: 0.032 m; data after Mayor et al. [10].

3. Slug flow simulator

3.1. Onset of the simulation

A given number of randomly distributed liquid slugs (and Taylor bubbles) is assumed to enter the column at its base. These distributed variables "introduce" in the simulation the effect of the gas injection system (in terms of the length of the gas bubbles and liquid slugs formed). The slug length (normal) distribution is prepared using Box Muller algorithm [16] and the bubble length distribution is prepared as a dependent distribution (i.e. a function of the slug length distribution). Assuming a cylindrical bubble shape, one can write:

$$U_G S_c \Delta t_i = S_b h_{b,i} \tag{3}$$

where Δt_i is the time interval required for the entrance in the column of the unit cell (i.e. bubble + slug), $h_{b,i}$ is length of bubble i and S_b and S_c stand for the bubble and the column cross sectional area, respectively. The estimate of S_b is computed based on the liquid film thickness determined following Brown [17] for free-falling conditions. At the column inlet, bubbles are assumed to rise at their undisturbed velocity, U_B^{exp}, and thus:

$$U_B^{exp} \Delta t_i = h_{b,i} + h_{s,i} \tag{4}$$

By combining the previous equations and rearranging one obtains:

$$h_{b,i} = \frac{h_{s,i}}{(S_b U_B^{exp}/S_c U_G) - 1} \tag{5}$$

The previous equation establishes the relation between the elements of the liquid slug distribution and the elements of the bubble length distribution that assure, at the column inlet, a given U_G and U_L (inputs to the simulation). The use of Eq. (5) for each unit cell allows thus to prepare the bubble length distribution as a function of the liquid slug length distribution. With the distributions of bubble length and liquid slug length at the column inlet, it is then possible to simulate the process of evolution of these distributions along the column.

3.2. Bubble motion along the column

The displacement of bubbles along the column is implemented as the incremental movement of their boundaries (bubble nose and rear). The position of the ith bubble rear, at instant t_{j+1}, $z_{rear,i}^{t_{j+1}}$, is computed by updating its position at t_j, $z_{rear,i}^{t_j}$, according to its velocity (U_i):

$$z_{rear,i}^{t_{j+1}} = z_{rear,i}^{t_j} + U_i(t_{j+1} - t_j) \tag{6}$$

The velocity of the bubble i (U_i) has two contributions: one related to the length of the liquid slug ahead of it (Eq. (1)), and another related to the expansion of the gas bubbles flowing below. This latter contribution will be described in detail in the following section. The position of the bubble nose is updated using:

$$z_{nose,i}^{t_{j+1}} = z_{rear,i}^{t_{j+1}} + h_{b,i}^{t_{j+1}} \tag{7}$$

Taking the boundaries of two consecutive bubbles, the length of the liquid slug flowing between them is given by:

$$h_{s,i}^{t_{j+1}} = z_{rear,i}^{t_{j+1}} - z_{nose,i+1}^{t_{j+1}} \tag{8}$$

Eqs. (6)–(8) are used for all bubbles flowing in the column, at every time increment.

3.3. Expansion of the gas phase along the column

As gas bubbles move upwards in the column, the pressure acting on each bubble decreases and, consequently, bubbles expand. Discarding the pressure drops in the liquid phase (at the wall and at the wake of the bubbles) the pressure along the column can be predicted taking only the hydrostatic pressure gradient. If one holds, then, the hydrostatic pressure at a given vertical coordinate, one can estimate the volume (or length) of a bubble, at that location, by using the *ideal gas law*. However, that computation requires an a priori knowledge of the number of moles of air in each bubble. This parameter can be assessed, for instance, at the base of the column (inlet position) where the hydrostatic pressure can easily be computed.

3.3.1. Evaluation of the amount of air in a bubble

Consider Fig. 2a representing the instant a bubble i enters the simulation domain. The fact that some bubbles are already inside the column, means the pressure acting on the bubble at the inlet, is smaller than it would be if the column was full of liquid. Furthermore, given that the axial pressure gradients along the (free-falling) liquid films are negligible and that the pressure recovery at the rear of the bubbles (when the liquid films slow down) is proportional to the amount of liquid in the films, one can compute the hydrostatic liquid height above a bubble i ($H_{hyd,i}$) taking only the liquid inside the column (as if the Taylor bubbles were removed from the column). Thus, for the scenario depicted in Fig. 2a, one can write:

$$H_{hyd,i} = z_{liq.} - \frac{S_b}{S_c} \sum_{k=1}^{i-1} h_{b,k} \tag{9}$$

where $z_{liq.}$ refers to the coordinate of the liquid free-surface.

Let us consider now the slightly more complex scenario of computing $H_{hyd,i}$ when one bubble is crossing the base of a tank (z_T) placed at the top of the column. This scenario is depicted in Fig. 2b. Given that the tank cross sectional area is considerably higher than the column's, it is reasonable to assume that the pressure at the base of the tank depends only on the height of liquid above that position ($z_{liq.} - z_T$), regardless of the presence of a bubble entering the tank (or even totally inside the tank). However, the portion of a bubble still inside the column (i.e. below z_T) should not be neglected when computing the hydrostatic liquid height above the bubble at the column inlet ($H_{hyd,i}$). The volume of liquid inside the column is reduced by the presence of a bubble crossing the tank base (or totally inside the column) and, consequently, the pressure acting on the bubble at the column inlet is also reduced. Thus, one must consider a new parameter, α_k, informing on the positioning of the bubbles

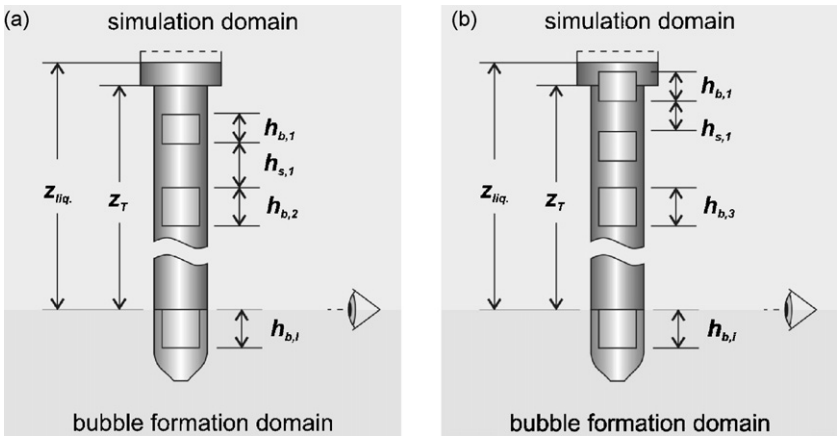

Fig. 2. Representation of the upward movement of a Taylor bubble at column inlet with (a) bubbles only inside the column and (b) bubbles entering the tank.

relative to the tank base. It should be defined as follows:

$$\text{bubbles totally inside the column} \Rightarrow \alpha_k = 1,$$

$$\text{bubbles crossing the tank base} \Rightarrow \alpha_k = \frac{z_T - z_{\text{rear},k}}{h_{b,k}},$$

$$\text{bubbles totally inside the tank} \Rightarrow \alpha_k = 0 \tag{10}$$

A more general form of Eq. (9) can, then, be written:

$$H_{\text{hyd},i} = z_{\text{liq.}} - \frac{S_b}{S_c}\sum_{k=1}^{i-1}(h_{b,k}\alpha_k) \tag{11}$$

which allows the computation of the hydrostatic liquid height above a bubble i, at the column inlet, in all possible scenarios (bubbles only inside the column; bubbles crossing the tank base; bubbles inside the column and inside the tank). For instance, the presence of a bubble totally inside the tank does not alter the pressure acting at the column inlet and, in agreement with this, the summation in the previous equation does not depend on the length of such a bubble (since $\alpha_k = 0$).

Having defined the hydrostatic liquid height above a bubble i at the inlet coordinate, the corresponding hydrostatic pressure can be computed as:

$$P_{\text{hyd},i} = \rho g H_{\text{hyd},i} \tag{12}$$

where ρ is the density of the liquid and g the acceleration of gravity. An algebraic transformation of the *ideal gas law* with further substitution of the pressure according to Eq. (12) yields an expression that computes the amount of air in a bubble i, at the inlet coordinate:

$$n_i = h_{b,i} S_b \frac{P_{\text{atm}} + \rho g H_{\text{hyd},i}}{RT} \tag{13}$$

where P_{atm} stands for ambient pressure, T refers to the temperature, R is the ideal gas constant and n_i is the number of moles of air in bubble i. Eq. (13) should be used for all bubbles entering the column in order to gather information on the number of moles of air in each bubble. This information is needed to predict the bubble length as bubbles move along the column. The following section addresses this issue.

3.3.2. *Effect over the length of the bubble*

Fig. 3 illustrates an instant in the upward movement of bubbles inside the simulation domain. The hydrostatic liquid height above bubble i is given by an expression similar to Eq. (11), with a correction to account for the positioning of the bubble ($z_{\text{nose},i}$)

$$H_{\text{hyd},i} = z_{\text{liq.}} - z_{\text{nose},i} - \frac{S_b}{S_c}\sum_{k=1}^{i-1}(h_{b,k}\alpha_k) \tag{14}$$

Taking Eq. (13) and transforming it to isolate $h_{b,i}$, one obtains

$$h_{b,i} = \frac{n_i RT}{S_b[P_{\text{atm}} + \rho g H_{\text{hyd},i}]} \tag{15}$$

where $H_{\text{hyd},i}$ is now given by Eq. (14). Knowing the positioning of a bubble i, Eq. (15) allows the computation of its length as a function of the hydrostatic pressure acting on it. This is not; however, a sequential calculation. The length of a bubble is a function of the vertical coordinate of the bubble nose (see Eq. (15)) whose computation, in turn, requires an estimate of the length of the bubbles (see Eq. (7)). This requires thus an iterative approach. After using Eq. (6) to update the positioning of every bubble rear, the "new" lengths of the bubbles are determined by iterating Eqs. (7), (14), (15) and (7), . . . until convergence is attained.

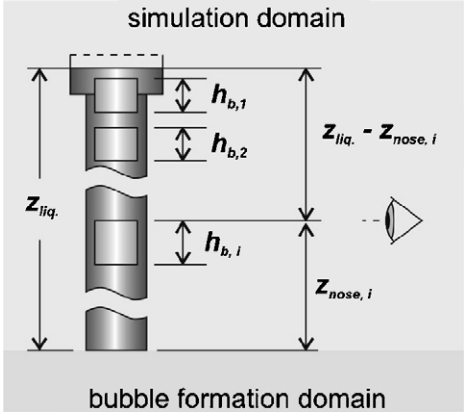

Fig. 3. Representation of the upward movement of a Taylor bubble inside the column.

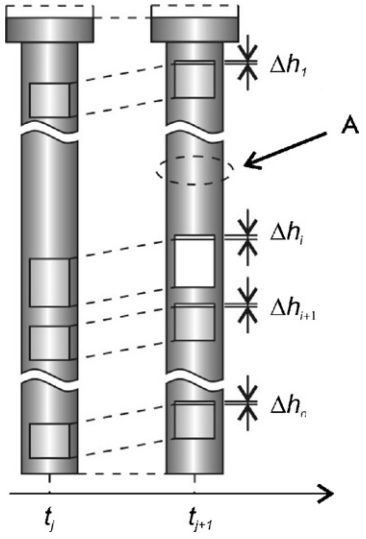

Fig. 4. Two consecutive moments in the upward movement of bubbles.

3.3.3. Effect over the velocity of the bubble

The bubble expansion is seen as a rise of the bubble nose region (reference frame attached to the bubble). Therefore, bubble expansion results in the upward displacement of everything ahead of the bubble (liquid and gas) by an amount proportional to the expansion of the bubble. Consider Fig. 4, representing the position of several bubbles, flowing upwards in a column, at instant t_j. Consider that, at instant t_{j+1} all bubbles had their positions updated according to their upward velocity (see Eq. (6)). The hydrostatic height above each bubble decreased from instant t_j to t_{j+1} and, therefore, all bubbles expanded accordingly (as described in the previous section).

Consider bubble i, in white in Fig. 4, and the liquid flowing ahead of it (zone A). The expansion of the bubbles under bubble i induces a raise in the liquid and gas ahead of them, proportional to the sum of the individual expansions undergone by each bubble ($\Delta h_1, \ldots, \Delta h_n$), and given by:

$$\Delta z_{\text{expans.}}^{\text{ahead } i} = \frac{S_\text{b}}{S_\text{c}} \sum_{k=i+1}^{n} \Delta h_k \tag{16}$$

This "extra" upward displacement of liquid and gas (Fig. 5) can be seen as an increase in the superficial liquid and gas velocities. This increase can be calculated dividing $\Delta z_{\text{expans.}}^{\text{ahead } i}$ by the time increment between the two consecutive instants under focus $(t_{j+1} - t_j)$, as in the following equation:

$$\Delta U_{\text{expans.}}^{\text{ahead } i} = \frac{\Delta z_{\text{expans.}}^{\text{ahead } i}}{t_{j+1} - t_j} = \frac{S_\text{b}}{(t_{j+1} - t_j) S_\text{c}} \sum_{k=i+1}^{n} \Delta h_k \tag{17}$$

where $\Delta U_{\text{expans.}}^{\text{ahead } i}$ is the increase in the flow velocity ahead of bubble i, due to the expansion of all bubbles flowing below it.

The upward velocity of gas bubbles flowing in a co-current liquid flow depends on the velocity profile in the liquid phase. This dependence is usually introduced by parameter C (equal to the ratio between the maximum and average liquid velocity), whose value depends on the flow regime (or velocity profile) in the liquid. Thus, the overall velocity of a bubble flowing in co-current flow is the result of two contributions: one related to the length of the liquid slug ahead of it (Eq. (1)), and another related to the "extra" upward displacement of the liquid and gas due to the gas phase expansion (Eq. (17)). The following equation allows the computation of the overall velocity of a bubble, i, in a train of bubbles flowing upwards:

$$U_i = U_\text{B}^{\text{exp}}[1 + 2.4\, \text{e}^{-0.8(h_{\text{s},i-1}/D)^{0.9}}] + \frac{C S_\text{b}}{(t_{j+1} - t_j) S_\text{c}} \sum_{k=i+1}^{n} \Delta h_k \tag{18}$$

where the experimental average upward bubble velocity is computed by a transformed version of Nicklin's equation:

$$U_\text{B}^{\text{exp}} = U_\infty + C(U_\text{L} + U_\text{G}^{\text{inlet}}) \tag{19}$$

where $U_\text{G}^{\text{inlet}}$, the superficial gas velocity at the inlet coordinate, is used instead of U_G in order to estimate the undisturbed upward bubble velocity discarding the effect of the gas phase expansion along the column. Recall that this effect is computed by the last parcel of the right hand side of Eq. (18). Correlation-based values of U_∞ and C (0.196 m/s and 1.2, respectively) were used in the simulations. The overall bubble velocity, given by Eq. (18), is used in Eq. (6) to update the positioning of bubble boundaries, implementing thus the bubble displacement.

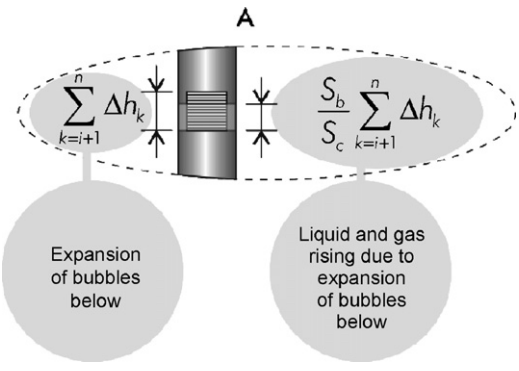

Fig. 5. Liquid and gas rise ahead bubble i due to the expansion of bubbles below it (zone A in Fig. 4).

4. Simulation results

Three major topics are addressed in this section: the validation/benchmarking of the simulator, the gas expansion along the column and the gas hold-up in the column.

4.1. Simulation validation/benchmarking

In this section, a brief comparison between experimental data and simulation results is shown, concerning two column internal diameters: 0.032 m and 0.024 m. The experimental data for the larger column is thoroughly described in Mayor et al. [10] while the data for the narrower column are taken from van Hout et al. [9,18]. The simulation results were obtained introducing at the inlet of the columns normal distributions of slug length ($\mu \approx 5D$

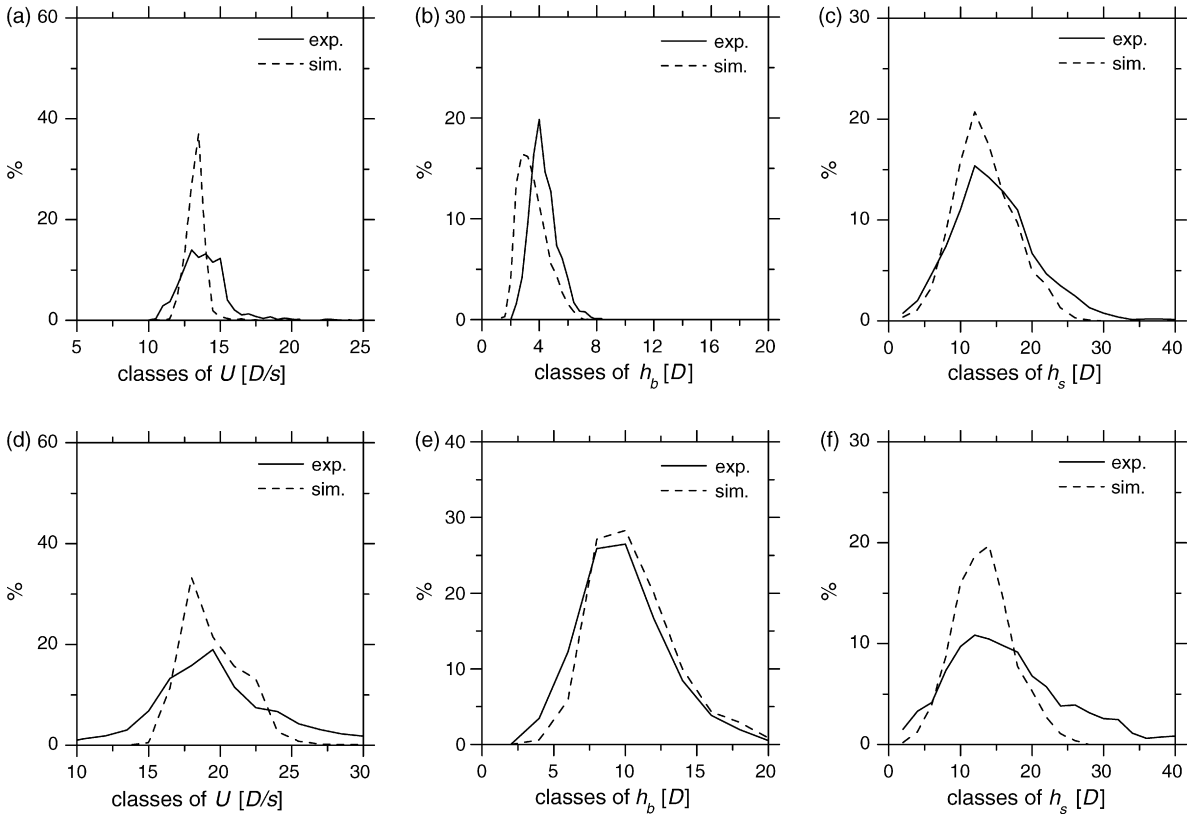

Fig. 6. Frequency distribution curves: (a) bubble velocity, (b) bubble length, (c) slug length, for an experiment/simulation with $U_L \approx 0.10$ m/s and $U_G \approx 0.088$ m/s; (d) bubble velocity, (e) bubble length, (f) slug length, for an experiment/simulation with $U_L \approx 0.10$ m/s and $U_G \approx 0.26$ m/s; 0.032 m ID; vertical coordinate: 5.4 m.

and $\sigma \approx 2D$). The characteristics of the inlet distributions were found, however, not to determine the flow pattern obtained at the column outlet (see Section 4.2).

Two different flow conditions ($U_L \approx 0.10$ m/s and $U_G \approx 0.088$ m/s; $U_L \approx 0.10$ m/s and $U_G \approx 0.26$ m/s) are addressed for the larger column (0.032 m, 6.5 m long). Fig. 6 shows the comparison for data at 5.4 m from the base of the column.

There is a very good agreement between experimental data and simulation results regarding the most probable value (mode) of the bubble velocity distributions (Fig. 6a and d), for both flow conditions. The corresponding standard deviations are, however, slightly different. The bubble length distributions from the simulations of both flow rate conditions represent the corresponding experimental data reasonably well (Fig. 6b and e). There is a slight underestimation, though, for the lower flow rate condition. The slug length distributions from the simulations of both flow conditions are in good agreement with the experimental data (Fig. 6c and f). Notice in particular the matching between the experimental and the simulation data for the most probable slug length value.

Fig. 7 shows the comparison between experimental and simulation data for the narrower column (0.024 m, 10 m long), regarding again two different flow conditions ($U_L \approx 0.01$ m/s and $U_G \approx 0.41$ m/s; $U_L \approx 0.10$ m/s and $U_G \approx 0.63$ m/s). The simulations are based on estimates of U_B^{exp} according to the Nicklin [3] correlation for co-current flow in turbulent regime (Eq. (2), with $C = 1.2$ and $U_\infty = 0.17$ m/s [6]). Focus is put on data at 6.88 m from the base of the column.

A very reasonable agreement between experimental data and simulation results is obtained, for both flow rate conditions, regarding the frequency distribution curves for bubble length (Fig. 7a and c) and for liquid slug length (Fig. 7b and d). The simulated frequency distribution curves from van Hout et al. [9,18] for the slug length variable are also shown in Fig. 7b and d (the curves were drawn directly from the charts of the mentioned publications). From the analysis of these curves it can be concluded that a better representation of the reported experimental data is obtained by using the simulator described in the present work.

In the light of the results discussed in this section, the proposed simulation approach emerges as a step towards a more accurate simulation of the slug flow pattern.

4.2. On the influence of the inlet slug length distribution

In a slug flow experiment, the characteristics of the flow pattern obtained at the column inlet depend on the type of gas injection system used. The gas injection systems influences, for instance, the mode and the standard deviation of the distributions of bubble length and liquid slug length obtained at that coordinate. Thus, different inlet distributions can be obtained using different gas injection systems. However, the differences in the inlet distributions tend to dissipate along the column due to coalescence. Furthermore, the length of column along which the influence of the different inlet distributions (the entrance effects) can be observed is usually known as the entrance length

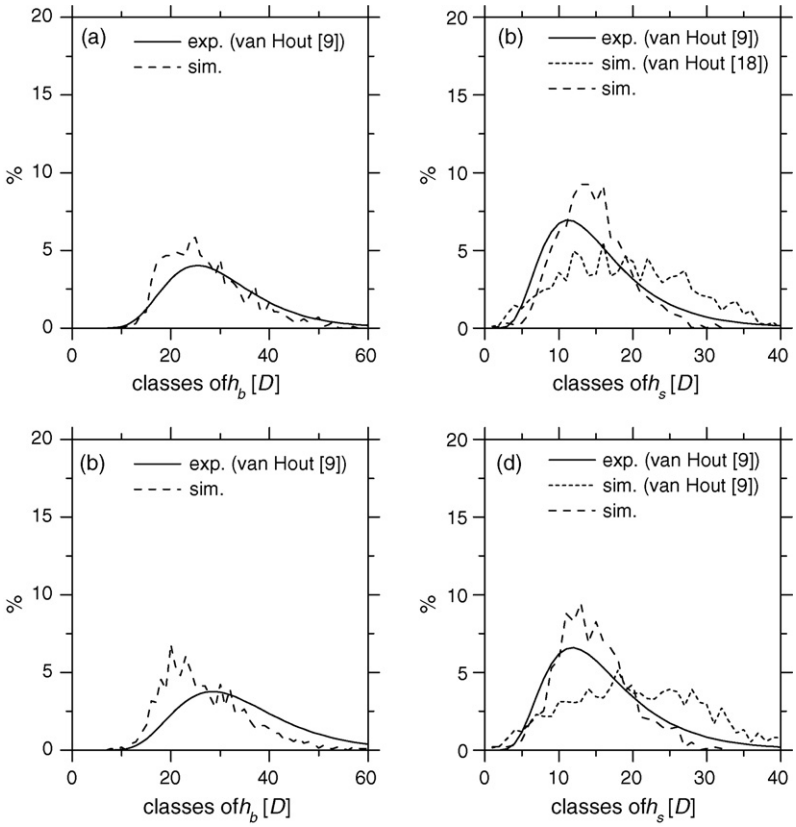

Fig. 7. Frequency distribution curves of (a) bubble length and (b) slug length, for an experiment/simulation with $U_L \approx 0.01$ m/s and $U_G \approx 0.41$ m/s; (c) bubble length and (d) slug length, for an experiment/simulation with $U_L \approx 0.10$ m/s, $U_G \approx 0.63$ m/s; 0.024 m ID; vertical coordinate: 6.88 m.

of slug flow. Note that we do not follow the terminology of some researchers that relate the entrance length to the column length required to have fully developed slug flow. The entrance length concept adopted here (related to the dissipation of the entrance effects) is based on the idea that different inlet flow patterns evolve along the column to a single flow pattern. The column length required to have the single flow pattern is highly relevant, for instance, when choosing the vertical (column) coordinate at which to validate the simulation algorithm.

For the purpose of studying the dissipation of the entrance effects along the column, three similar simulations were performed for a 6.5 m long column (0.032 m ID). These differed only in the slug length distributions introduced at the column inlet. Three normal distributions centred on 2*D*, 5*D* and 8*D* were considered. Their evolution along the column was monitored at several observation points (in steps of 0.6 m). The frequency distribution curves of h_b and h_s obtained, for each simulation, at each observation point, were compared schematically. The

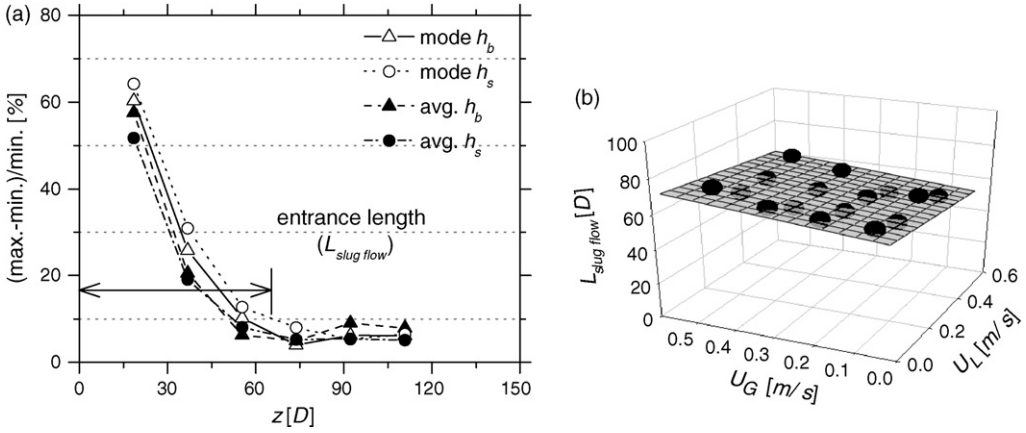

Fig. 8. (a) Maximal relative difference of the mode and average (h_b and h_s) along the column, for simulations with increasing average inlet slug lengths (2*D*, 5*D* and 8*D*), $U_L \approx 0.10$ m/s and $U_G \approx 0.26$ m/s; (b) entrance length of slug flow for simulations with U_L and U_G equal to 0.10, 0.23, 0.36 and 0.50 m/s; 0.032 m ID.

maximum relative differences between those curves (focussing the average and the mode) are plotted against the vertical coordinate of the column in Fig. 8a. This figure confirms that the inlet differences dissipate along the column. Despite the differences in the inlet distributions, similar frequency distribution curves are obtained for vertical column positions above 65*D*, when $U_L \approx 0.10$ m/s and $U_G \approx 0.26$ m/s (accepting a maximal difference of 10%). 65*D* is thus the entrance length of the slug flow for the mentioned operating conditions (U_L and U_G). Extending the aforementioned approach to a set of increasing superficial gas and liquid velocities, one obtains the chart of Fig. 8b, showing the entrance length of slug flow for U_G and U_L in the range 0.10–0.50 m/s. For this range, the entrance length of slug flow varies between 50*D* and 70*D*. Note that the two vertical coordinates at which the experimental data were collected (3.25 and 5.40 m, i.e. 102*D* and 169*D*, respectively) are far above the mentioned entrance-length range. Thus, no entrance effects are likely to be affecting the experimental data collected. In addition, the fact that the simulation results above 70*D* are free from entrance effects (i.e. not dependent on the particular flow pattern characteristics at the column inlet), and that those results are in good agreement with the obtained experimental data (Section 4.1), is a further corroboration of the accurateness, robustness and usefulness of the proposed simulator.

4.3. On the gas expansion inside the column

4.3.1. Effect of gas expansion over bubble coalescence

A singular simulation was done in order to isolate the effect of the gas phase expansion over the flow development along the column. Non-distributed liquid slug lengths were considered at the inlet of the column, and the bubble-to-bubble interaction was discarded. The former constrain assures that every liquid slug (and gas bubble) enters the column featuring equal length. Additionally, the fact that no bubble-to-bubble interaction is implemented in the upward movement of the bubbles guarantees that any evolution of the flow characteristics can be ascribed to the gas phase expansion. The simulation refers to a 6.5 m long column with 0.032 m internal diameter, equipped with a large cross sectional tank at the column outlet. In Fig. 9, the length of bubbles (h_b) and liquid slugs (h_s) and the velocity of bubbles (U) are plotted against the column vertical coordinate, for a given instant after the start-up of a simulation.

The origin of the vertical coordinate (horizontal axis) is positioned at the base of the column. The expansion of the gas phase is computed only above that position. Above the column inlet, and due to the onset of the gas expansion, the bubble and slug lengths and the bubble velocity increase along the column.

Although the increase in the length of the bubbles (above inlet) can be directly related to the expansion of the gas phase, a deep analysis of all effects influencing the flow pattern is required to fully interpret the variation of the liquid slug length along the column (increasing slightly). According to Eq. (18), the velocity of a bubble *i* flowing in the column has a contribution related to the expansion of the bubbles flowing below (last parcel of the right hand side of the equation). This means that

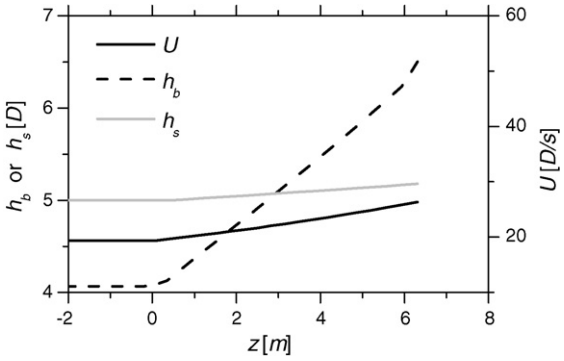

Fig. 9. Bubble length, slug length and bubble velocity along the vertical coordinate of the column, for a given instant (simulation discarding bubble-to-bubble interaction and with constant lengths of bubbles, slugs and bubble velocity at the inlet).

the first bubble (from top to bottom), of a train of bubbles flowing in the column, has its velocity affected by the expansion of more bubbles than does, for instance, the second bubble (flowing below the first). Consequently, this "extra" velocity, due to expansion, is higher for the first bubble than for the second bubble, which is, in turn, higher than for the third bubble, and so on. These ordered relations ($U_1 > U_2 > U_3$, ..., clearly perceivable in Fig. 9) lead to the increase in the length of the liquid slugs as the train of bubbles flow upwards (see Fig. 9). This shows, therefore, that the gas expansion phenomenon slightly "opposes" to the merging of consecutive bubbles (coalescence) as it induces the increase (though smooth) in the length of the slugs. It is, nevertheless, a limited effect.

The fact that gas phase expansion has limited influence over the phenomenon of bubble coalescence points out a possible strategy for further assessing the correctness of the gas expansion algorithms proposed in Section 3.3. Under this assumption it is reasonable to expect that an approximate flow simulation, performed without gas expansion along the vertical coordinate, produce, at a given vertical coordinate, average flow parameters (such as bubble length, bubble velocity or liquid slug length) that are similar to those obtainable by a simulation featuring gas expansion. However, this matching is only likely to happen when the U_G estimate introduced in the approximate simulation (without gas phase expansion) is corrected for the pressure at the vertical coordinate in question. To compute that, one must have information on the gas hold-up inside the column. For this purpose, the average gas hold-up was computed based on instantaneous gas hold-ups obtained at every second of the simulation including gas expansion. Three types of simulations were then performed: one considering gas expansion as described previously and two approximate approaches based on U_G estimates corrected for the mid- and top-column pressure, respectively. These two approaches are, ultimately, often implemented in many gas–liquid systems (e.g. [7,8,11]). All simulations regard the flow in 6.5 m long columns with 0.032 m internal diameter, equipped with a large cross sectional tank at the column outlet. The comparison focuses on the average liquid slug length (Fig. 10a and b), bubble length (Fig. 10c and d) and bubble velocity (Fig. 10e and f), at two vertical coordinates in the column

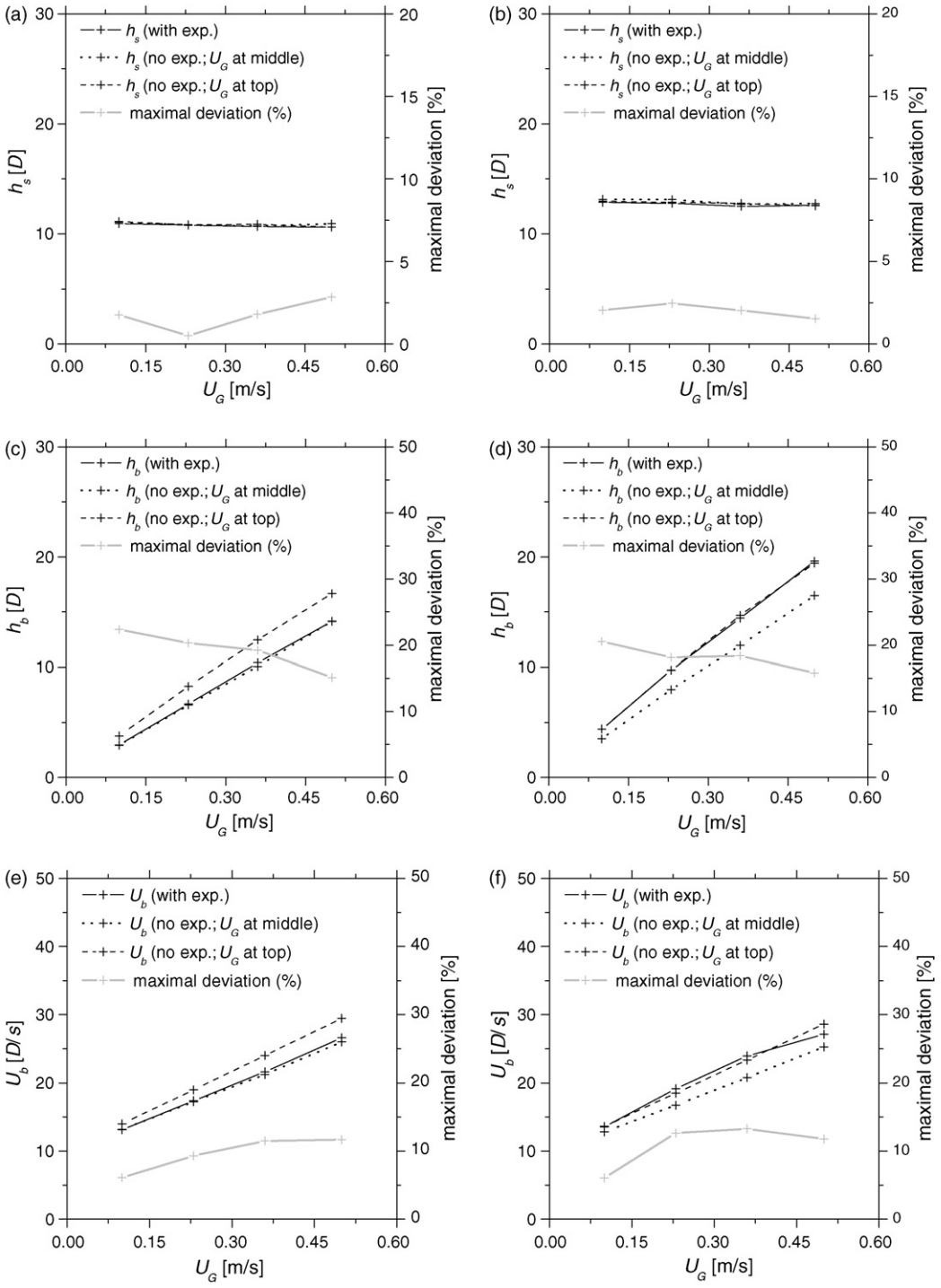

Fig. 10. Average liquid slug length (a and b), bubble length (c and d) and bubble velocity (e and f) for simulations considering expansion (varying U_G) and discarding expansion (constant U_G equal to value at the middle or at the top of the column); $U_L = 0.10$ m/s and $U_G = 0.10$, 0.23, 0.36 and 0.50 m/s; column length: 6.5 m; outlet configuration: large tank; (a), (c) and (e) vertical coordinate: 3.25 m; (b), (d) and (f) vertical coordinate: 6.40 m.

(3.25 and 6.40 m, charts on the left and on the right, respectively). A superficial liquid velocity equal to 0.10 m/s and superficial gas velocities in the range 0.10–0.50 m/s were used.

As evident in the charts of Fig. 10a and b, all three types of simulations (with and without gas expansion) produce very similar average liquid slug lengths. Indeed, the maximal relative deviation between these approaches reaches no more than 3%, for both column vertical coordinates, and for the ranges of U_L and U_G studied. This is in agreement with the results of Fig. 9, as it confirms that the evolution of slug length variable is not strongly affected by gas expansion. Fig. 10c–f presents similar comparisons focussing on the average bubble length and velocity. It is possible to observe that, for both variables and at the two vertical coordinates, the simulation including gas expansion produces average results very similar to those obtained for the approximate simulations based on U_G estimates at the pressure

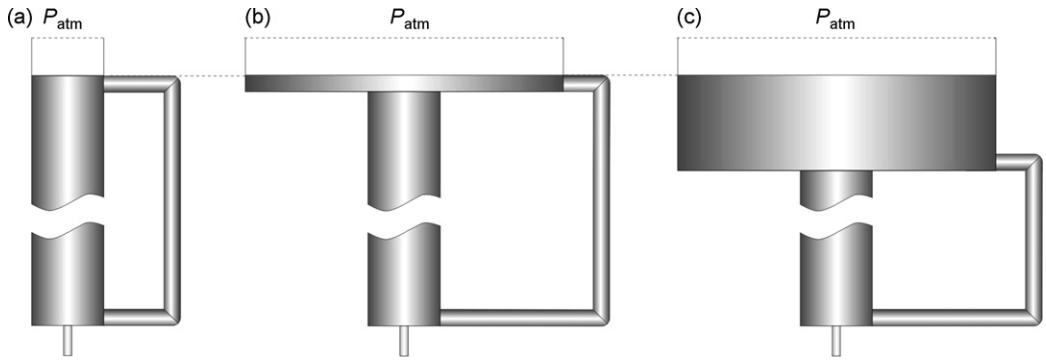

Fig. 11. Column outlet configurations: (a) no tank, (b) flat large cross sectional tank and (c) regular large cross sectional tank.

of the corresponding vertical coordinate. For instance, in Fig. 10c (data at the mid-column coordinate), the results of the simulation featuring gas expansion match those for the simulation based on U_G estimates corrected for the mid-column pressure. It is also possible to observe that, the simulations based on U_G values corrected for pressure other than that of the corresponding vertical coordinate, originate rather different estimates of the average bubble length and velocity. For the chosen vertical coordinates (and corresponding U_G estimates), deviations of up to 22% and 12% were obtained for bubble length and bubble velocity, respectively. This fact was expected since gas expansion is known to play an important role in the evolution of these variables.

The results discussed here confirm, as postulated previously, the correctness of the proposed gas expansion algorithms. They provide, in addition, further corroboration that the gas phase expansion does not have a pronounced effect over the coalescence of bubbles along the column.

4.3.2. Relevance of gas expansion implementation in the assessment of flow parameters

As already discussed, it is possible to obtain reasonable average estimates of the flow parameters (such as h_b, U_b or h_s) even when simulating slug flow without gas expansion along the column, provided that the U_G value introduced in the simulation is corrected for the pressure at the vertical coordinate in question. This is, however a very unpractical procedure (when compared to the simulation including expansion along the column) since one simulation is required for every desired vertical coordinate. In addition, the correction of the U_G estimates for the pressure at a given vertical coordinate requires, as already mentioned, information on the average gas and liquid retention inside the column (in order to calculate the hydrostatic pressure at that coordinate). And still, this information may not be always available. Indeed, although gas hold-up values can be assessed, during a given slug flow experiment, by stopping the flow momentarily in order to measure the amount of liquid inside the column, this only provides for instantaneous estimates of gas hold-up. Therefore, a correction of U_G based on such instantaneous (as opposed to average) gas hold-up estimate is accomplished with some degree of inaccuracy, which may result finally in the more or less inaccurate computation of the average flow parameters.

Finally, the implementation of the gas phase expansion along the column is a step towards a more accurate simulation of slug flow pattern. It enables a deeper study of the dynamic evolution of the flow and promotes a wider understanding of its governing rules.

4.3.3. Effect of the outlet configuration on the gas expansion rate

The expansion of gas bubbles along the column is a function of the hydrostatic pressure acting on the bubbles, which is, in turn, dependent on the coordinate of the liquid free-surface, among other parameters (see Eqs. (14) and (15)). Considering that the outlet configuration of the column influences the coordinate of the liquid free surface (dampening effect), it is interesting to assess the extent of the influence of the outlet configuration over the gas expansion in the column. Three configurations are addressed: a column without a tank at the top (Fig. 11a), a column with a flat large cross sectional tank at the top (Fig. 11b) and a column with a regular large cross sectional tank at the top (Fig. 11c). These scenarios are discussed in the following sections.

4.3.3.1. Column without a tank at the top (outlet). The flow in a 6.5 m long column with internal diameter of 0.032 m was simulated considering superficial liquid and gas velocities (U_L and U_G) equal to 0.25 and 0.36 m/s, respectively. Gas superficial velocity is given at ambient pressure. Gas expansion and bubble-to-bubble interaction is considered in the simulation. Focus is put on the evolution of the velocity of the first bubble along time. Notice that the so-called first bubble in the column changes every time a bubble reaches the liquid free-surface (second bubble becomes the new first bubble). The velocity of the first bubble (comprising and discarding gas expansion) is plotted against time in Fig. 12.

As expected, the velocity of the first bubble discarding the gas expansion contribution is constant and equal to the undisturbed upward bubble velocity as computed in Eq. (19). However, if the gas expansion contribution is considered, the evolution of the velocity of the first bubble is rather interesting. There is a continuous increase in U_1 in the first seconds of the simulation, followed by an oscillatory behaviour. The initial escalation of U_1 is related to the fact that the simulation starts with the column full of liquid (no bubbles inside the column). As bubbles enter the column (increasing gas hold-up) the first bubble of the

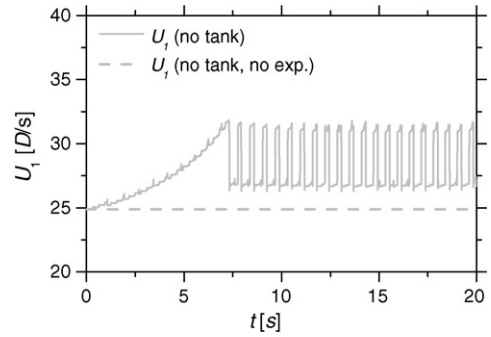

Fig. 12. Values of the velocity of the first bubble along time for a simulation with $U_L \approx 0.25$ m/s and $U_G \approx 0.36$ m/s; without a tank at the column outlet.

train is affected by the expansion of an increasing number of bubbles. Therefore, there is a continuous escalation of U_1 due to the increase in the last parcel of the right hand side of Eq. (18). This increase continues until the first bubble reaches the liquid free-surface. From that moment onward, an oscillatory behaviour is observed. In order to fully understand the causes of this behaviour special attention must be put in the evolution along time of other parameters, as bubbles reach the liquid free-surface. Those parameters are the vertical coordinates of the liquid free-surface and of the nose of the first bubble, as well as the hydrostatic liquid height above the first bubble. These parameters are plotted against time in Fig. 13 (in the range 15–16.5 s).

Consider an instant *a* at which the first bubble of a train of bubbles reaches the liquid free-surface. At that instant, this interface, previously at 6.5 m (outlet coordinate) from the base of the column, drops instantly by an amount proportional to the height of the bubble exiting the column. Moreover, there is an "apparent" sudden drop in the coordinate of the nose of the first bubble, since the new first bubble (previously second bubble) is flowing somewhere below in the column. From that moment onward, the liquid free surface will rise steadily due to the continuous entrance of gas and liquid in the column. This rise

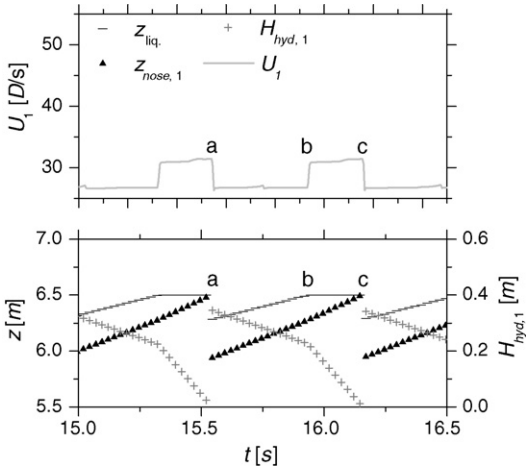

Fig. 13. Plot of velocity and nose coordinate of the first bubble (U_1 and $z_{nose,1}$), hydrostatic liquid height above first bubble ($H_{hyd,1}$) and vertical coordinate of the liquid free-surface ($z_{liq.}$) along time, in the range 15–16.5 s; simulation with $U_L \approx 0.25$ m/s and $U_G \approx 0.36$ m/s; without a tank at the column outlet.

will continue until the liquid reaches again the outlet system (at 6.5 m from the base of the column; instant *b*). At the same time, the new first bubble will rise in the column until it reaches the liquid free-surface (at instant *c*). Considering that the hydrostatic liquid height above the first bubble is calculated as the difference between the liquid free-surface coordinate ($z_{liq.}$) and the bubble nose coordinate ($z_{nose,1}$), it is obvious that this parameter has different variation rates in time intervals *a–b* and *b–c*. The movement of the liquid free surface, in the time interval *a–b*, accounts for this difference. As a direct consequence of the different variation rate of the pressure acting on the bubbles in these time intervals, different expansion rates occur. Indeed, the expansion of all bubbles flowing in the column between instants *a* and *b* is smaller than between instants *b* and *c*. As a consequence, the expansion contribution for the velocity of the first bubble (but also for the remaining bubbles), in the former time interval is smaller than in the latter time interval. The aforementioned oscillatory behaviour of U_1 is, therefore, the result of the dynamic evolution of the liquid free-surface coordinate.

4.3.3.2. Column with a flat large cross sectional tank at the top (outlet). A large cross sectional tank is often used at the top of the columns to assure proper separation of gas and liquid phases. Moreover, besides phase separation, such a tank has the advantage of strongly decreasing the oscillation of the liquid free-surface. Considering that the liquid free-surface oscillation originates considerable variations in the velocity of the bubbles inside the column (as discussed in the previous section), it is interesting to investigate if the dampening effect of a large cross sectional tank affects also the evolution of the bubble velocity inside the column. For this purpose, the operating conditions addressed in the previous section were simulated again considering the existence of a flat large cross sectional tank at the top of the column. The tank cross sectional area is large enough so as to assure a practically constant liquid free-surface. The velocity of the first bubble (with and without gas expansion) is plotted against time in Fig. 14a and b.

As expected, a constant value is obtained when the gas expansion contribution is withdrawn from U_1. However, when focussing on the overall U_1 (including expansion contribution) a puzzling result emerges. Although the evolution of U_1 is, most of the time, strongly dampened when compared to the same parameter for the no-tank scenario (see Fig. 14b), intriguing negative values of velocity are attained at every instant following bubble burst events (when bubbles reach the liquid free-surface). As before, a closer analysis of several parameters is required in order to shed light on this peculiar behaviour. These are the nose and rear coordinate of first and second bubbles, their velocities and lengths, and the corresponding hydrostatic liquid height. A short time range (15.0–16.5 s) is covered in Fig. 15.

For easier interpretation of the chart, both the first and second bubbles are depicted, at a given moment, in the chart. As these bubbles flow upwards in the column, the hydrostatic liquid height above them decreases and, accordingly, their lengths escalate. At instant *a*, the first bubble reaches the liquid free-surface and bursts. The previous second bubble becomes then the first bubble. As the volume of the bursting bubble is

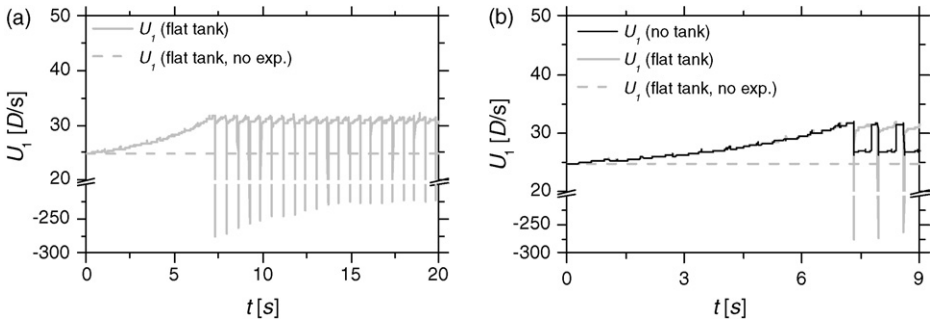

Fig. 14. Values of the velocity of the first bubble along time for a simulation with $U_L \approx 0.25$ m/s and $U_G \approx 0.36$ m/s; (a) range: 0–20 s, flat tank data; (b) range: 0–12 s, no tank and flat tank data.

replaced, instantly, by liquid from the upper tank, there is a sudden increase in the pressure acting on the "new" first bubble, previously the second bubble. This abrupt escalation in pressure is the result of the equally abrupt change in the hydrostatic liquid height acting on the bubble ($H_{\mathrm{hyd},1}^{\mathrm{after}\,a} > H_{\mathrm{hyd},2}^{\mathrm{before}\,a}$; note that despite the change in indexes these parameters refer to the same bubble). As a consequence of pressure escalation, bubble contraction, perceived as a decrease in bubble length, occurs ($h_{\mathrm{b},1}^{\mathrm{after}\,a} < h_{\mathrm{b},2}^{\mathrm{before}\,a}$, as evident in the upper chart of Fig. 15). This sudden bubble contraction, which obviously spans all bubbles in the column, occurs at every bubble burst event. Moreover, the extent of contraction decreases from the top to the base of the column, an expected behaviour since the variation of gas volume with pressure decreases as pressure escalates (see Eq. (15)). Given that, as discussed previously (Section 3.3.3), bubble expansion results in an upward displacement of everything ahead of the bubble (the "extra" velocity due to expansion), bubble contraction, on the contrary, results in a downward displacement of the flow (a negative "extra" velocity). Indeed, a plunge of the gas and liquid inside the column occurs at every bubble burst event, resulting in the momentary negative bubble velocities shown in the charts of Figs. 14 and 15. This plunge is very brief and a regular evolution of bubble velocity is obtained in the subsequent instants. Notice that these negative peaks in bubble velocities are related to the assumption of instantaneous column refilling (with liquid from the tank) at bubble burst events. In addition, the amplitude of these negative peaks must only be addressed in conjunction with the chosen simulation time increment, since the truly meaningful parameter is the plunging length of the first bubble (equal to $U_1 \times t_{\mathrm{incr.}}$). Notice additionally that the instantaneous column refilling assumption, reasonable for low viscosity fluids (such as water for instance), might not be adequate if high viscosity fluids are to be considered. In that scenario, the overall evolution of the gas phase inside the column would result from the balance between gas phase contraction (more or less pronounced depending on the time required for column refilling), and the gas expansion related to the upward movement of the bubbles (due to the decreasing hydrostatic pressure). Parameters such as liquid viscosity and column diameter would play an important role in the aforementioned balance since they affect the time required for column refilling.

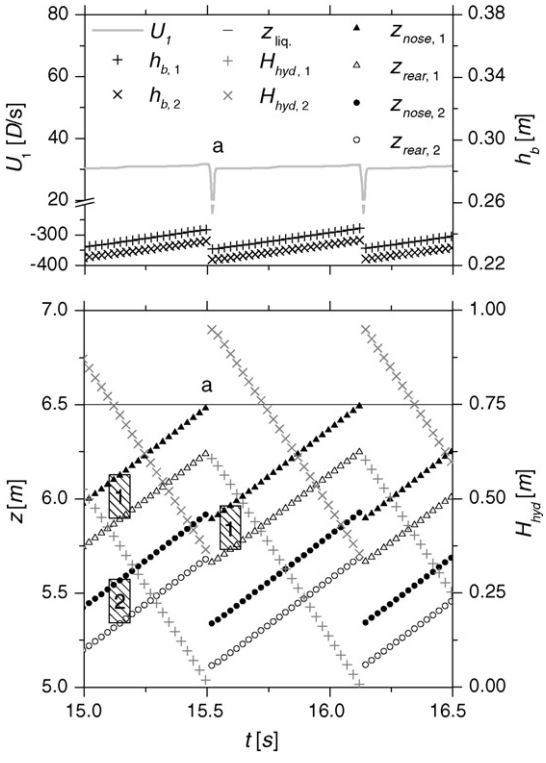

Fig. 15. Plot of nose and rear coordinates of the first and second bubbles ($z_{\mathrm{nose},1}$, $z_{\mathrm{rear},1}$, $z_{\mathrm{nose},2}$ and $z_{\mathrm{rear},2}$), hydrostatic liquid height above first and second bubbles ($H_{\mathrm{hyd},1}$ and $H_{\mathrm{hyd},2}$), length of first and second bubbles ($h_{\mathrm{b},1}$ and $h_{\mathrm{b},2}$), velocity of first bubble (U_1) and vertical coordinate of the liquid free-surface ($z_{\mathrm{liq.}}$) along time, in the range 15.0–16.5 s; simulation with $U_L \approx 0.25$ m/s and $U_G \approx 0.36$ m/s; with a large flat tank (0.01 m height) at the column outlet.

The use of a flat large cross sectional tank at the top of the column assures a practically steady liquid free surface and, most of the time, strongly dampened bubble velocities (and expansion rate). However, as a drawback, it brings about more or less pronounced instantaneous drops on bubble velocities (and expansion rate) at every bubble burst event. Nevertheless, the attainment of a steady liquid free-surface, often crucial in real applications (in which structural instabilities related to bubble bursting are undesirable, for instance), is, by itself, a strong incentive for the further development of the large tank solution. The use of an alternative tank configuration is discussed in the following section.

4.3.3.3. Column with a regular large cross sectional tank at the top (outlet). As an attempt to overcome the recurrent plunging

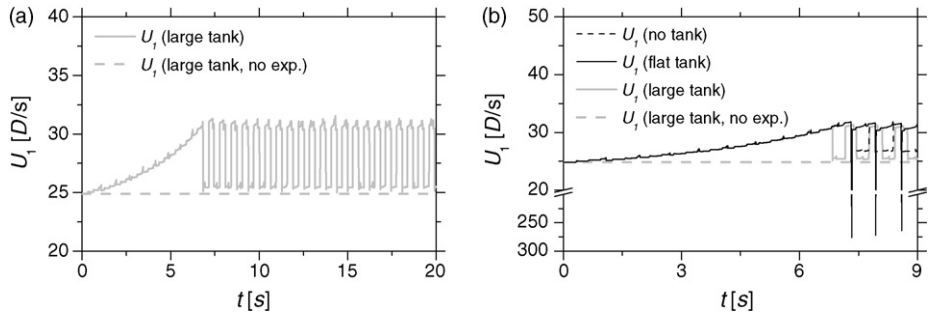

Fig. 16. Values of the velocity of the first bubble along time for a simulation with $U_L \approx 0.25$ m/s and $U_G \approx 0.36$ m/s; (a) range: 0–20 s, large tank data; (b) range: 0–12 s, no tank, flat tank and large tank data.

of the flow at bubble burst events, an alternative tank has been tested. The tank cross sectional area is similar but its height is considerably larger (0.5 m instead of the previous 0.01 m). It is hypothesised that by having a tank height higher than the length of the bubbles reaching the liquid free surface, the pressure change inside the column due to bubble burst events should be less abrupt. For this purpose, the operating conditions addressed in the previous sections were simulated again acknowledging now the new tank configuration. The velocity of the first bubble (with and without gas expansion) is plotted against time in Fig. 16.

As expected, a constant value is obtained when the gas expansion contribution is withdrawn from U_1 (Fig. 16). Moreover, the recurring plunging of the flow, described previously for the flat tank configuration, is no longer present (no negative values of overall velocity). However, the evolution of the first bubble velocity is akin to the evolution for the no tank configuration (Fig. 16b). There is, as for that configuration, an intermittent oscillation between two major velocity values.

As before, a closer analysis of some parameters is required to expound the reasons for this behaviour. These are the vertical coordinates of the nose and rear of the first bubble, in particular in the vicinity of the base of the tank (vertical coordinate $z_T = 6$ m), and the hydrostatic liquid height above the second bubble, $H_{hyd,2}$. The variation of these parameters is plotted against time (in the range 15–16.5 s) in Fig. 17.

Three different time instants are relevant for the understanding of the oscillations of U_1: instant a referring to the moment at which a first bubble reaches the liquid free surface ($z = 6.5$ m); instants b and c referring to the moments at which the nose and rear of a "new" first bubble, respectively, reach the base of the tank ($z = 6.0$ m). Notice that instant a is prior to instants b and c because, after the burst of a first bubble at instant a, the previously second bubble, flowing somewhere below, becomes the "new" first bubble. Unlike the simulation with no tank at the top of the column, no major change in the velocity of the first bubble is observed when a bubble reaches the liquid free surface (instant a, in Fig. 17). The large cross sectional tank at the top of the column assures that the coordinate of the liquid free surface remains practically unchanged at that event. Therefore, the evolution of the hydrostatic pressure acting on the "old" second bubble is fairly steady during the burst of the first bubble ($P_{hyd,2}^{\text{before } a} \approx P_{hyd,1}^{\text{after } a}$; as already mentioned, despite the change in indexes these parameters refer to the same bubble). Attention must be focused now on the evolution of the hydrostatic liquid height above the second bubble ($H_{hyd,2}$), along time. The variation rate (slope) of this parameter between instants a and b is fairly constant (negative but almost constant). However, at instant b there is a sudden change in the variation rate (slope) of $H_{hyd,2}$. Between instants b and c the first bubble is crossing the base of the tank and, as a consequence, the last parcel of the right hand side of Eq. (14) is smaller than before instant b ($\alpha_1 = 1$ before instant b, and decreasing from 1 to 0 between instants b and c). As a result, the variation rate (slope) of $H_{hyd,2}$ in that time interval is less steep (than in the time interval a–b) and, consequently, the corresponding bubble expansion is smoother. The original variation rate of $H_{hyd,2}$ is observed again as soon as the rear of the first bubble is above the tank base (after instant c, and until the next burst event; $\alpha_1 = 0$ in that time interval). Notice that this analysis has been focused on the hydrostatic liquid height above the second bubble just for the sake of simplicity. Similar effects occur for all the bubbles in the column, although with different extent. Thus, because all bubbles in the

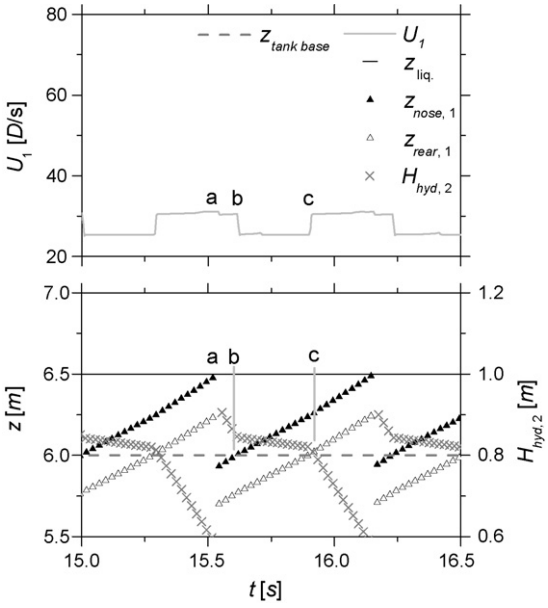

Fig. 17. Plot of nose and rear coordinates and velocity of the first bubble ($z_{nose,1}$, $z_{rear,1}$, U_1), hydrostatic liquid height above second bubble ($H_{hyd,2}$) and vertical coordinate of the liquid free-surface ($z_{liq.}$) along time, in the range 9–11 s; simulation with $U_L \approx 0.25$ m/s and $U_G \approx 0.36$ m/s; with a large tank at the column outlet (0.5 m height).

column expand less when the first bubble of the train of bubbles is crossing the base of the tank, a smaller gas expansion rate is obtained inside the column during those periods, which result finally in the oscillation of the bubble velocities (and hence the oscillations in U_1).

By increasing the height of the outlet tank (for values higher than bubble lengths) one avoids the sudden pressure change at bubble burst events of the flat tank configuration, but continues to have pressure oscillation, though more gradual, as bubbles reach the base of the bank. The advantages of the regular large tank configuration (large in terms of cross sectional area as well as height) are thus two-fold: while it assures an almost steady liquid free-surface (which can be important for several practical applications), it prevents the flow plunging of the flat tank configuration. However, as already mentioned it does not avoid some degree of oscillation in the expansion rate of the gas phase.

4.4. On the gas hold-up inside the column

The retention of gas inside the column, usually termed gas hold-up, is one of the most important parameters for the hydrodynamic characterization of two-phase flows. It is defined as the fraction of gas inside the column and can be computed by v_G/v in terms of volume (or alternatively by H_G/H, in terms of the corresponding column equivalent heights; note that $v_G = H_G S_c$). Considering that v_G escalates along the column as the gas phase expands, and that the rate at which this happens is influenced by the column outlet configurations, it is interesting to study how these parameters/phenomena interrelate. For this purpose two approaches are pursued: one addressing the effect of the column outlet configuration over the average value of gas hold-up and another assessing the relevance of the gas phase expansion in the estimation of average gas hold-up. The outcome of these approaches is discussed in the following sections.

4.4.1. Effect of the outlet configuration on the average gas hold-up

Several simulations were performed considering, as before, the flow in a 6.5 m long column with internal diameter of 0.032 m. Superficial liquid and gas velocities equal to 0.10, 0.23, 0.36 and 0.50 m/s were set. Every operating condition was simulated for each of the three outlet configurations described previously (see Fig. 11). The average gas hold-up obtained for simulations featuring no tank at the column outlet (Fig. 11a) is plotted against the superficial liquid and gas velocities in Fig. 18. The average gas hold-up is based on several hundreds of instantaneous gas hold-up values obtained at every second of the simulations.

As expected, gas hold-up escalates for increasing superficial gas velocity and for decreasing superficial liquid velocity. This derives from its definition (H_G/H) and from flow continuity. Moreover, similar behaviour is obtained for the remaining outlet configurations (flat and large tank). In Fig. 19 the average gas hold-up is plotted against U_G, for the three outlet configurations (no tank, flat tank and large tank) and U_L equal 0.10 and 0.50 m/s (the extreme values of the range).As perceivable in the chart of this figure, fairly similar gas hold-ups are obtained with the three outlet configurations for the highest superficial liquid velocity ($U_L = 0.50$ m/s). The deviation between the obtained gas hold-ups increases with U_G but reaches no more than 2%. However, this deviation increases for decreasing U_L. For instance, for U_L equal to 0.10 m/s, the deviation between the gas hold-ups obtained for the three outlet configurations reaches 6%. Moreover, and although not shown for the sake of simplicity, the maximum deviations (occurring for $U_G = 0.50$ m/s) are about 2, 3, 4 and 6% when U_L is equal to 0.50, 0.36, 0.23 and 0.10 m/s, respectively. These are nevertheless limited deviations, and match in particular the operating conditions leading to a higher gas fraction inside the column (i.e. high U_G/U_L ratio).

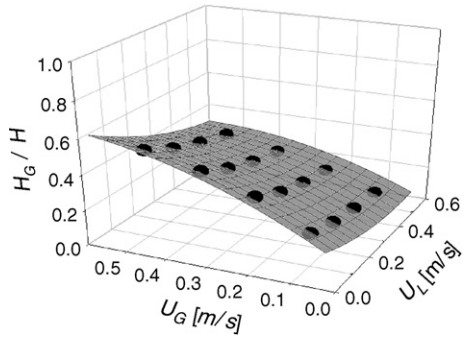

Fig. 18. Gas hold-up for simulations with U_L and U_G equal to 0.10, 0.23, 0.36 and 0.50 m/s; no tank at the column top (Fig. 11a); column length: 6.5 m; surface fit equation: $H_G/H = 0.59(U_L)^2 - 0.60U_L - 0.82(U_G)^2 + 1.31U_G - 0.53U_L U_G + 0.14$, $r^2 = 0.998$.

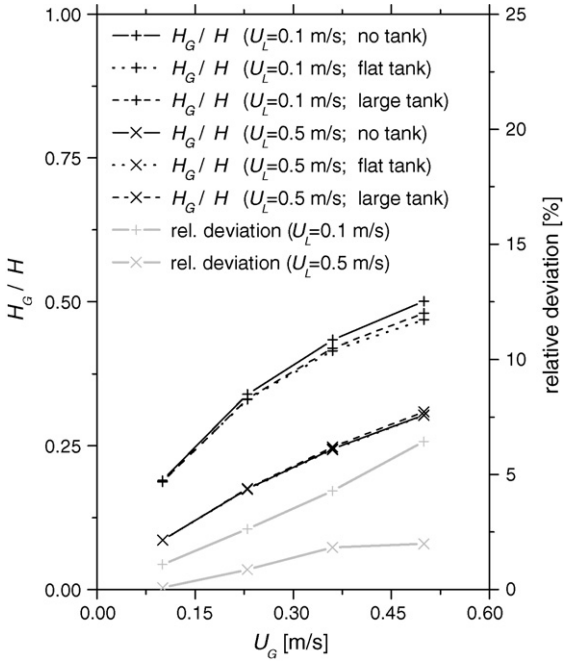

Fig. 19. Gas hold-up for simulations with different column top configurations (no tank, flat tank and large tank); $U_L = 0.10$ and 0.50 m/s; $U_G = 0.10$, 0.23, 0.36 and 0.50 m/s; column length: 6.5 m.

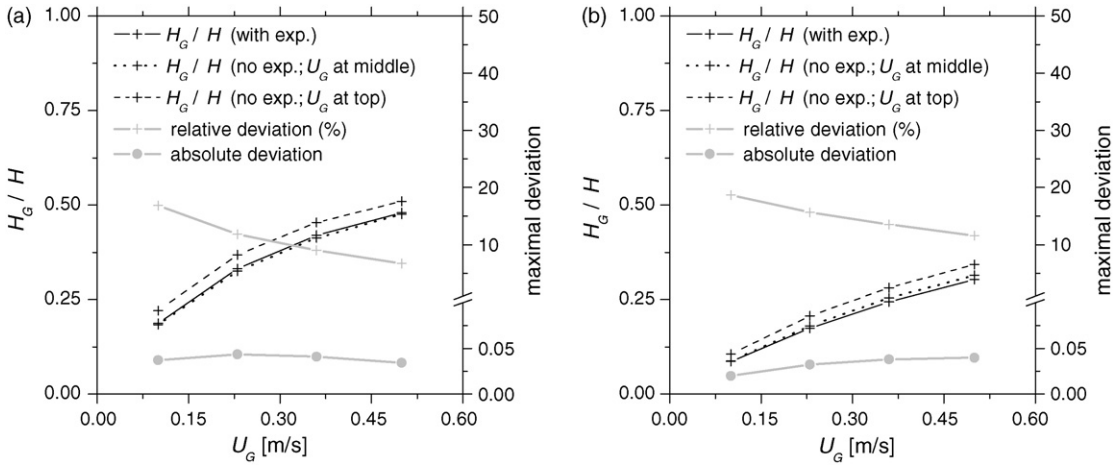

Fig. 20. Gas hold-up for simulations considering expansion (varying U_G) and discarding expansion (constant U_G equal to value at the middle or at the top of the column): (a) $U_L = 0.10$ m/s and (b) $U_L = 0.50$ m/s; for $U_G = 0.10$, 0.23, 0.36 and 0.50 m/s; column length: 6.5 m; outlet configuration: large tank.

4.4.2. Relevance of gas expansion implementation in the assessment of gas hold-up

An attempt is made to gauge the relevance of the gas expansion in the computation of the gas hold-up. Following a strategy discussed previously, a comparison is made between three types of simulations: one including gas expansion and two others discarding gas expansion. For these approximate approaches, estimates of U_G are introduced in the simulations after correction for the pressure at the middle and at the top of the column, respectively. The three outlet configurations mentioned before were tested in each approach. The gas hold-up obtained for the large tank configuration is plotted against U_G in Fig. 20 (for U_L equal to 0.10 and 0.50 m/s).

The charts of this figure indicate that even when no gas expansion is considered in the simulation, it is still possible to compute the average gas hold-up with reasonable accuracy, provided that the estimate of U_G introduced in the simulator is corrected for the pressure at the middle of the column. Indeed, in that situation, the relative deviation between the gas hold-up of the simulations including expansion and the approximate approach (discarding expansion) is always smaller than 4%, for the ranges of U_G and U_L studied (0.10–0.5 m/s). Notice that the gas hold-up values (given in %) of both approaches differ less than 1 percentage point. However, when the estimate of U_G is introduced in the simulation at ambient pressure, higher gas hold-up deviations are obtained. For the ranges of U_G and U_L studied the relative deviations vary in the ranges 6–15% ($U_L = 0.10$ m/s) and 12–19% ($U_L = 0.50$ m/s). Notice that the relative deviations decrease for increasing U_G and decreasing U_L (Fig. 20), i.e. for increasing gas hold-up. Nevertheless, the gas hold-up values of the two approaches differ just by 2–4 percentage points.

The previous approach was also implemented for simulations based on a longer column (20 m long). The results obtained for the large tank configuration are shown in Fig. 21.

As for the shorter column, a reasonable evaluation of the gas hold-up is obtained for simulations discarding the gas phase expansion provided that the U_G estimate is given at the mid-column pressure. For that situation, the relative deviations obtained are smaller than 5%. Moreover, quite like for the shorter column, the corresponding gas hold-up values differ less than 1 percentage point. In opposition to this, quite significant relative deviations exist between the simulation including gas expansion and the approximate simulation, when U_G is used at the ambient pressure. These deviations vary in the range 16–34% (for $U_L = 0.10$ m/s and U_G in the range 0.10–0.50 m/s). Notice that for the same operating conditions, the deviations obtained for the 6.5 m long column are less than half of those obtained for the 20 m long column. It is therefore evident that as column length increases it becomes more and more inadequate to compute gas hold-up by the simpler approach discussed (no expansion along the column and U_G at ambient pressure) (Fig. 21).

The previous discussion was based only on the large tank configuration just for the sake of simplicity. Similar conclusions derive from simulations based on the other outlet configurations.

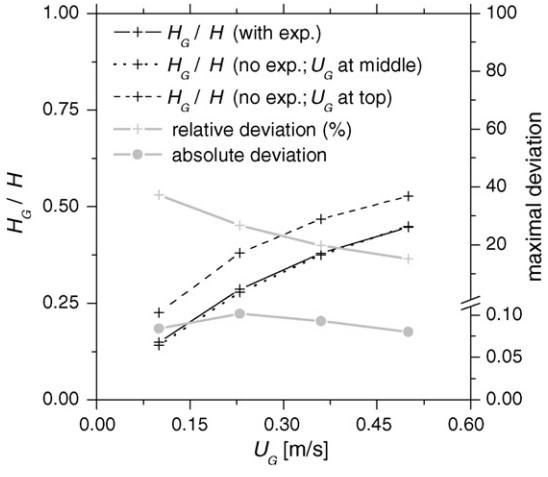

Fig. 21. Gas hold-up for simulations considering expansion (varying U_G) and discarding expansion (constant U_G equal to value at the middle or at the top of the column); $U_L = 0.10$ m/s and $U_G = 0.10$, 0.23, 0.36 and 0.50 m/s; column length: 20 m; outlet configuration: large tank.

5. Conclusions

A simulation study on the gas phase expansion and gas hold-up in co-current slug flow is reported. The simulations including gas expansion and approximate approaches are shown to produce very similar estimates of the average liquid slug length. Similar matching can be observed regarding the average bubble velocity and length, provided that the U_G estimates, used in the approximate approaches, are corrected for the vertical coordinate in question. In agreement with this, the gas phase expansion is shown to have reduced influence over the coalescence of bubbles (gas expansion slightly decreases coalescence).

The influence over the gas expansion rate of three alternative outlet configurations is discussed. The first, featuring no tank at the column outlet, brings along strong oscillations of the gas expansion rate and, consequently, of the bubble velocities. The second configuration, featuring a flat large cross sectional tank at the column outlet, assures most of the time, a strongly dampened gas expansion rate (and hence bubble velocities) but, as a drawback, leads to recurrent plunging of the flow inside the column, at every bubble burst event. The third configuration, implying a regular large and high cross sectional tank at the column outlet, prevents this latter phenomenon and stabilises the liquid free surface. It does not avoid, however, some degree of oscillation in the expansion rate of the gas phase, much alike the one observed for the no tank configuration.

As expected, the average gas hold-up is shown to escalate with increasing U_G and decreasing U_L. The column outlet configurations are shown to have reduced effect over the average gas hold-up (deviations smaller than 6% for U_L and U_G in the range 0.10–0.50 m/s). Approximate approaches based on U_G values corrected for the pressure at the middle of the column are shown to produce good estimates of the average gas hold-up (deviations smaller than 5%) for the ranges of U_L, U_G and H studied. Approximate approaches based on the U_G at ambient pressure are shown not to produce good estimates of the average gas hold-up, especially as column length increases.

Acknowledgments

The authors gratefully acknowledge the financial support of Fundação para Ciência e a Tecnologia through project POCTI/EQU/33761/1999 and scholarship SFRH/BD/11105/2002. POCTI (FEDER) also supported this work via CEFT.

Appendix A. Nomenclature

C	empirical coefficient
D	column internal diameter (m)
g	acceleration of gravity (m s^{-2})
h_b (h_s)	length of bubble (slug) (m)
Δh_i	expansion of bubble i (m)
H_G (H)	height of gas (and liquid) inside the column (m)
$H_{hyd,i}$	hydrostatic liquid height above bubble i (m)
n	number of bubbles (#)
n_i	number of moles of air of bubble i (mol)
P_{atm}	ambient pressure (Pa)
$P_{hyd,i}$	hydrostatic pressure on buble i (Pa)
R	universal gas constant (J K^{-1} mol^{-1})
S_b (S_c)	bubble (column) cross section area (m^2)
t_j, t_{j+1}	consecutive time instants (s)
T	temperature (K)
U_b	bubble velocity (m s^{-1})
U_B (U_∞)	upward bubble velocity (drift velocity) (m s^{-1})
U_G (U_L)	superficial gas (liquid) velocity (m s^{-1})
U_i	bubble i upward velocity (m s^{-1})
v_G(v)	volume of gas (and liquid) inside the column (m^3)
z (z_T)	vertical coordinate of the column (tank base) (m)
$z_{liq.}$	liquid free-surface coordinate (m)
z_{nose} (z_{rear})	vertical coordinate of bubble nose (rear) (m)

Greek letters

α_i	parameter informing on the bubble positioning relative to the tank base
ρ	density of liquid (kg m^{-3})

References

[1] D.T. Dumitrescu, Stromung an Einer Luftblase im Senkrechten Rohr, Z. Angeus. Math. Mec. 23 (1943) 139–149.
[2] R.M. Davies, G.I. Taylor, The mechanics of large bubbles rising through extended liquids and through liquids in tubes, Proc. R. Soc. Lond., A 200 (1950) 375–392.
[3] D.J. Nicklin, J.O. Wilkes, J.F. Davidson, Two-phase flow in vertical tubes, Trans. Inst. Chem. Eng. 40 (1962) 61–68.
[4] R. Collins, F.F. De Moraes, J.F. Davidson, D. Harrison, The motion of large gas bubble rising through liquid flowing in a tube, J. Fluid Mech. 28 (1978) 97–112.
[5] J. Fabre, A. Liné, Modeling of two-phase slug flow, Ann. Rev. Fluid Mech. 24 (1992) 21–46.
[6] E.T. White, R.H. Beardmore, The velocity of single cylindrical air bubbles through liquids contained in vertical tubes, Chem. Eng. Sci. 17 (1962) 351–361.
[7] D. Barnea, Y. Taitel, A model for slug length distribution in gas–liquid slug flow, Int. J. Multiphas. Flow 19 (1993) 829–838.
[8] H.A. Hasanein, G.T. Tudose, S. Wong, M. Malik, S. Esaki, M. Kawaji, Slug flow experiments and computer simulation of slug length distribution in vertical pipes, AIChE Symp. Ser. 92 (1996) 211–219.
[9] R. Van Hout, D. Barnea, L. Shemer, Evolution of statistical parameters of gas–liquid slug flow along vertical pipes, Int. J. Multiphas. Flow 27 (2001) 1579–1602.
[10] T.S. Mayor, Studies on the hydrodynamics of gas-liquid flows: slug flow regime, PhD Thesis, Chemical Engineering Department, Porto University, 2007.
[11] M.N. Coelho Pinheiro, A.M.F.R. Pinto, J.B.L.M. Campos, Gas hold-up in aerated slugging columns, Chem. Eng. Res. Des. 78 (2000) 1139–1146.
[12] R. Seyfried, A. Freundt, Experiments on conduit flow and eruption behavior of basaltic volcanic eruptions, J. Geophys. Res. 105 (2000) 23727–23740.
[13] B. Chouet, P. Dawson, T. Ohminato, M. Martini, G. Saccorotti, F. Giudicepietro, G. De Luca, G. Milana, R. Scarpa, Source mechanisms of explosions at Stromboli volcano, Italy, determined from moment-tensor inversions of very-long-period data, J. Geophys. Res. 108 (2003) 2019, doi:10.1029/2002JB001919.
[14] M.R. James, S.J. Lane, B. Chouet, J.S. Gilbert, Pressure changes associated with the ascent and bursting of gas slugs in liquid-filled vertical and inclined conduits, J. Volcanol. Geoth. Res. 129 (2004) 61.

[15] T.S. Mayor, A.M.F.R. Pinto, J.B.L.M. Campos, An image analysis technique for the study of gas–liquid slug flow along vertical pipes-associated uncertainty, Flow Measur. Instrum., in press.
[16] R. Campos Guimarães, J.A. Sarsfield Cabral, Estatística, McGraw-Hill, de Portugal Limitada, 1997.
[17] R.A.S. Brown, The mechanics of large gas bubbles in tubes. I. Bubble velocities in stagnant liquids, CJChE 43 (1965) 217–223.
[18] R. Van Hout, L. Shemer, D. Barnea, Evolution of hydrodynamic and statistical parameters of gas–liquid slug flow along inclined pipes, Chem. Eng. Sci. 58 (2003) 115–133.